Common Base Four-Finger InGaAs/InP Double Heterojunction Bipolar Transistor with Maximum Oscillation Frequency 535 GHz *

NIU Bin(牛斌)[12], WANG Yuan(王元)[1], CHENG Wei(程伟)[1**], XIE Zi-Li(谢自力)[2], LU Hai-Yan(陆海燕)[1], CHANG Long(常龙)[1], XIE Jun-Ling(谢俊领)[1]

[1]*Science and Technology on Monolithic Integrated Circuits and Modules Laboratory, Nanjing Electronic Devices Institute, Nanjing 210016*

[2]*Key Laboratory of Advanced Photonic and Electronic Materials, Department of Physics, Nanjing University, Nanjing 210093*

(Received 28 February 2015)

A common base four-finger InGaAs/InP double heterojunction bipolar transistor with 535 GHz $f_{\max}$ by using the 0.5 μm emitter technology is fabricated. Multi-finger design is used to increase the input current. Common base configuration is compared with common emitter configuration, and shows a smaller K factor at high frequency span, indicating a larger breakpoint frequency of maximum stable gain/maximum available gain (MSG/MAG) and thus a higher gain near the cut-off frequency, which is useful in THz amplifier design.

PACS: 73.40.Kp, 85.30.De, 71.55.Eq DOI: 10.1088/0256-307X/32/7/077304

Recently, research in devices working in terahertz bands (300 GHz–3 THz) has become a booming thread, due to its extensive potential applications, such as spectroscopy, imaging and communications.[1] Due to the high saturated drift velocity of electrons in InP/InGaAs, InP-based transistors are particularly suitable for THz applications compared with other materials. High frequency performances of InP heterojunction bipolar transistors (HBTs) and high-electron mobility transistors (HEMTs) have been improved rapidly. To date, maximum oscillation frequencies of both the types of InP based transistors have exceeded 1 THz.[2–6]

Compared with InP HEMTs, InP HBTs tend to have higher breakdown voltage, higher threshold uniformity, lower $1/f$ noise, and higher digital speed, making them more suitable for sub millimeter and future THz electronics.

Common-emitter (CE) configuration is frequently used nowadays in sub-millimeter amplifier design. However, according to recent research,[7] InP double heterojunction bipolar transistors (DHBTs) in common-base (CB) configurations can yield a much higher power gain at high frequency, especially near the cutoff frequency. Their maximum stable gain (MSG) extends into higher frequencies in common base than in common emitter configuration.

In this Letter, we present a common base four-finger InGaAs/InP DHBT, fabricated with a triple mesa process and a benzocyclobutene (BCB) planarization technique. All processes were carried out on 3-inch wafers. The area of each emitter finger is $0.5\times7\,\mu\text{m}^2$. The maximum oscillation frequency $f_{\max}$ is 535 GHz and the breakdown voltage BV_{CBO} is 4 V.

The superiority of CB configuration can be seen from the following calculations.[8] In an ideal case, when Rollet's stability factor K becomes larger than unity, MAG (G_{MA}) of InP HBT can be written as

$$G_{\text{MA}} = G_{\text{MS}}/(K+\sqrt{K^2-1}), \tag{1}$$

where G_{MS} is the MSG of the device. The K factor has a different expression between CB and CE configuration,

$$K^{(\text{CB})} \cong \Big(R_{\text{B}}+2R_{\text{E}}+2R_{\text{C}} + \frac{2R_{\text{E}}R_{\text{C}}}{R_{\text{B}}}\Big)\omega C_{\text{bci}}+\omega\tau_{\text{F}}, \tag{2}$$

$$K^{(\text{CE})} \cong \Big(R_{\text{E}}+2R_{\text{B}}+2R_{\text{C}}+\frac{2R_{\text{B}}R_{\text{C}}}{R_{\text{E}}}\Big)\omega C_{\text{bci}} + \Big(1+\frac{2R_{\text{B}}}{R_{\text{E}}}\Big)\omega\tau_{\text{F}}, \tag{3}$$

$$K^{(\text{CE})}-K^{(\text{CB})} = \frac{2R_{\text{B}}}{R_{\text{E}}}\omega\tau_{\text{F}}+(R_{\text{B}}-R_{\text{E}}) \cdot\Big(1+2\frac{R_{\text{B}}+R_{\text{E}}}{R_{\text{B}}R_{\text{E}}}R_{\text{C}}\Big)\omega C_{\text{bci}}, \tag{4}$$

where R_{B}, R_{E} and R_{C} are the effective base, emitter and collector resistances respectively, C_{bci} is the intrinsic base-collector capacity, τ_{F} is the total forward carrier transit time. From Eq. (4) we can see that when $R_{\text{B}} \geq R_{\text{E}}$, which is often the actual case, $K^{(\text{CE})}$ is larger than $K^{(\text{CB})}$. Thus the InP HBT in CE configuration reaches its MSA/MAG breakpoint frequency $f_{K=1}$ faster than in the CB configuration. Consequently, the CB configuration can yield a much higher $f_{\max}$.

The epitaxial layer of the DHBT was grown on a 3-inch semi-insulating InP substrate by using molecular-beam epitaxy (MBE). The layered structure is shown

*Supported by the National Basic Research Program of China under Grant No 2011CB301900, and the Natural Science Foundation of Jiangsu Province under Grant Nos BK2011010 and BY2013077.

**Corresponding author. Email: dspbuilder@163.com

© 2015 Chinese Physical Society and IOP Publishing Ltd

in Table 1. First, a 200 nm Si-doped n^+ InGaAs sub-collector layer was grown. Above the collector contact layer, a 150 nm n-type InP collector was grown. An InGaAs set-back layer followed by a δ-doping InP layer was grown on the base side of the collector. The composite collector layer was designed to eliminate the conduction band spike at B–C interface and to minimize the collector current blocking effect.[9] A 35 nm carbon-doped p^+ InGaAs base was grown. Finally, a 200 nm n^+ InP emitter and a 200 nm n^+ InGaAs cap layer were grown.

After material epitaxy, a four-finger CB DHBT device was fabricated. The geometry was defined by using i-line stepper lithography. Three mesas were formed through selective wet-etching. The base contact metal was defined by using the self-aligned technique. Ti/Pt/Au was used as the emitter-collector contact, while Pt/Ti/Pt/Au was used as the base contact. All metals were formed through deposition and lift-off processes. Metal posts were made to connect contacts with pads. After device isolation, the planarization process was performed by using BCB, which also acts as the passivation layer. Following an RIE etch-back process, pad metal was formed, and the device process was finished.

Table 1. Layered structure of the InGaAs/InP DHBT.

Layers	Material	Thichness (nm)	Dopant
Emitter Contact	InGaAs	200	Si
Emitter	InP	200	Si
Base	InGaAs	35	C
Set-back	InGaAs	30	Si
δ-doping	InP	20	Si
Collector	InP	150	Si
Collector Contact	InGaAs	50	Si
Sub-collector	InP	200	Si
Etch-stop	InGaAs	10	ud
InP substrate			S.I.

As shown in Fig. 1(a), four emitter fingers were designed in two rows. In each row, two fingers were aligned with 7 μm interval. The area of each emitter finger is $0.5 \times 7\,\mu m^2$. Distributing the total emitter area into four fingers can avoid a long emitter, in which it is hard to maintain uniform current along the emitter and it may cause degradation of performance.

Compared with the previous four-finger InGaAs/InP DHBT result reported in Ref. [7], the emitter width is narrowed from 1 μm to 0.5 μm, which can effectively reduce the emitter junction area, leading to a smaller emitter junction capacity C_{be} and intrinsic base-collector capacity C_{bci}.

To analyze the differences between CB and CE experimentally, we fabricated a common emitter four-finger InGaAs/InP DHBT using the same technology, as shown in Fig. 1(b). Each finger has an emitter area of $0.5 \times 7\,\mu m^2$.

To improve the high frequency performance, base resistance R_{bb} as long as intrinsic collector capacity C_{bci} should be reduced. Base resistance can be expressed as

$$R_{bb} = R_{b,cont} + R_{b,gap} + R_{b,spread}, \quad (5)$$

where $R_{b,cont}$, $R_{b,gap}$ and $R_{b,spread}$ are base contact resistance, base-emitter gap resistance and spread resistance beneath emitter junction respectively, $R_{b,cont}$ was reduced through suppressing base contact resistivity ρ_c. Using the self-align process can reduce $R_{b,gap}$ effectively. Narrowing the emitter width can reduce $R_{b,spread}$ as long as the intrinsic collector capacity C_{bci}. A low base sheet resistor ρ_s can also help to reduce $R_{b,gap}$ and $R_{b,spread}$. According to the TLM test results, we achieve ρ_c of $1.48\,\Omega\cdot\mu m^2$ and ρ_s of $736\,\Omega/\square$, leading to a base resistance as small as 3.81 Ω in this work.

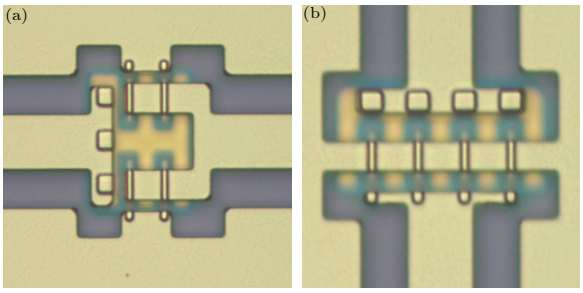

Fig. 1. Microscope pictures of the four-finger InGaAs/InP DHBT (a) in the CB configuration and (b) in the CE configuration.

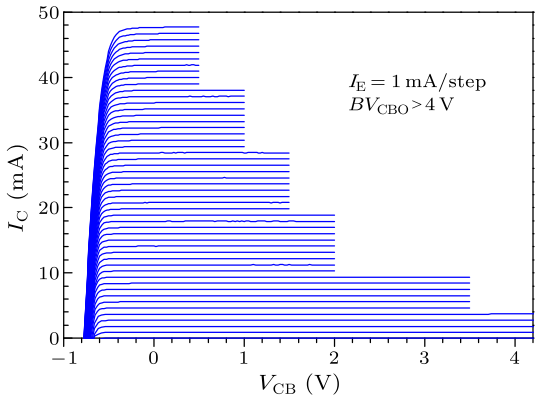

Fig. 2. The I–V characteristics of the common base four-finger InGaAs/InP DHBT.

The common-base four-finger InGaAs/InP DHBT was characterized on wafer at room temperature. The dc characteristics were measured by using an Agilent 1500 A semiconductor parameter analyzer. As shown in Fig. 2, when the emitter current rises from 1 mA to 50 mA, the knee voltage increases from −0.6 V to −0.3 V. The offset voltage is about −0.8 V. The breakdown voltage is over 4 V, which is defined at an emitter current density of $10\,\mu A/\mu m^2$.

Different from the I–V curves in CE configuration, the offset voltage and the knee voltage in the CB configuration stretch into the minus part of V_{CB} span, which indicates that the inner electric field caused by space charges is large enough to compensate for

the reverse applied voltage. The small value and the sharp rising of the knee voltage indicate that the current blocking effect caused by the discontinuity of conduction band has been successfully suppressed by our composite collector design.[9]

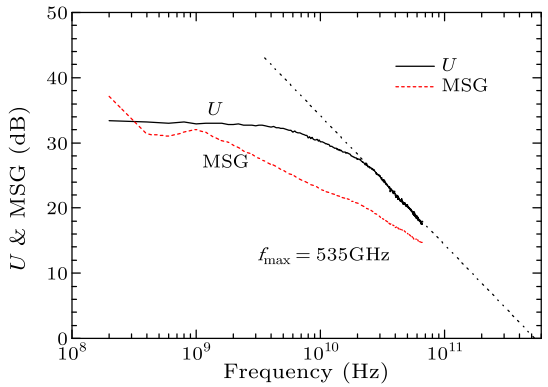

Fig. 3. The values of MSG/MAG and U of the common base four-finger DHBT at $V_{CE} = 1.1$ V and $I_C = 60$ mA.

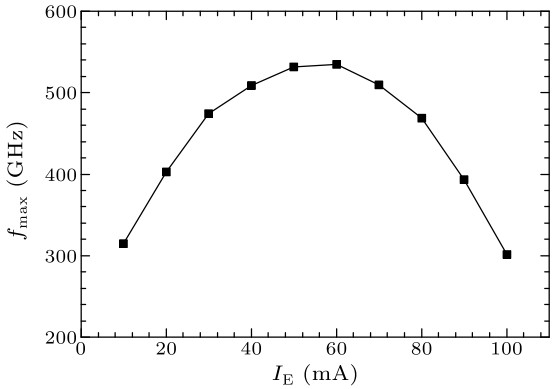

Fig. 4. The value of f_{max} versus I_E of the common base four-finger DHBT.

Although CB has no current gain, it has a larger voltage swing owning to a low knee voltage and a high breakdown voltage, due to the fact that $BV_{CBO} > BV_{CEO}$ is often the case. Compared with Ref. [7] we measured a BV_{CBO} over 4 V. It makes the four-finger InP DHBT suitable for a power amplifier.

S-parameter of the common-base four-finger InGaAs/InP DHBT was characterized from 200 MHz to 67 GHz, by using a PNA-X N5247A network analyzer. Open/short pads identical to devices' pads were designed to de-embed the pad parasitic, thus accurate microwave performance of the device can be induced. Due to the common-base configuration, current gain is always less than unity. Therefore no current gain cutoff frequency (f_t) can be induced. The maximum oscillation frequency (f_{max}) can be extrapolated through two methods. One is maximum stable gain/maximum available gain (MSG/MAG), the other is Mason's unilateral gain (U). The maximum oscillation frequency is defined as the frequency when MSG/MAG or U drops to unity. Mason's unilateral power gain can be calculated by

$$U = |Y_{21} - Y_{12}|^2/[4(G_{11}G_{22} - G_{21}G_{12})], \quad (6)$$

where G_{11}, G_{12}, G_{21} and G_{22} are the real parts of the network's Y-parameters.

Both MSG/MAG and U from 200 MHz to 67 GHz were depicted in Fig. 3. The MSG rolls at -10 dB/decade and the slope of MAG is not fixed, while U has a constant slope of -20 dB/decade.[11] Thus we used U to extrapolate f_{max} rather than MSG/MAG, and the extrapolated f_{max} is 535 GHz. The value of f_{max} is higher than recent reports in Ref. [7] due to its small intrinsic base-collector capacity C_{bci} and base resistance R_{bb} as discussed above.

The value of f_{max} of the common base four-finger DHBT changes with emitter current I_E, as shown in Fig. 4. Here f_{max} increases from 315 GHz to the top 535 GHz as I_E increases from 10 mA to 60 mA. From 60 mA to 100 mA, f_{max} drops to 300 GHz as a consequence of the Kirk effect.

The K factor, which affects the breakpoint of MSG/MAG, can be extracted as follows:

$$\Delta = S_{11}S_{22} - S_{12}S_{21}, \quad (7)$$

$$K = \frac{1 - |S_{11}|^2 - |S_{22}|^2 + |\Delta|^2}{2|S_{12}S_{21}|}. \quad (8)$$

The extracted K factor for CB and CE devices are illustrated in Fig. 5. When $f > 4$ GHz, the K factor of the CE device begins to increase with the frequency, and reaches 0.87 at 67 GHz. On the other hand, the K factor of the CB device continues to decrease until 53 GHz, and shows a trend to increase, reaching -0.19 at 67 GHz. We can speculate that the CE device's K factor reaches unity much faster than CBs, which corresponds with our prediction. Thus a higher gain near cutoff frequency for the CB device could be expected.

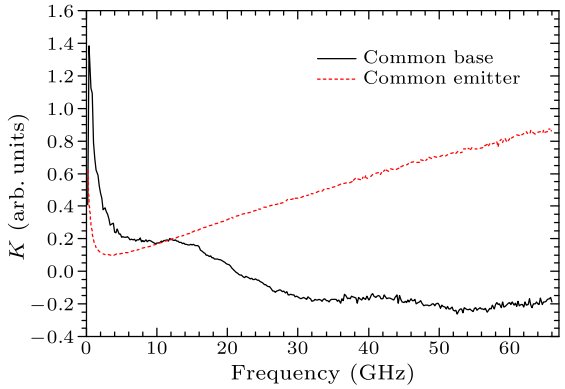

Fig. 5. The values of K and Δ of the CB and CE four-finger DHBTs at $V_{CE} = 1.1$ V and $I_C = 60$ mA.

In conclusion, a four-finger submicron InGaAs/InP DHBT in common base configuration has been presented. Narrowed emitter line width and reduced base contact are helpful to improve f_{max} to 535 GHz. A common base configuration is used and a smaller K

factor at the high frequency is demonstrated, indicating a larger MSG/MAG breakpoint frequency and thus a higher gain when the frequency reaches the MAG region of common emitter devices, which is helpful in THz applications.

References

[1] Samoska S 2006 *IEEE MTT-S Int. Microwave Symp. Dig.* (San Francisco, USA 11–16 June 2006) p 333

[2] Lai R, Mei X B, Deal W R, Yoshida W, Kim Y M, Liu P H, Lee J, Uyeda J, Radisic V, Lange M, Gaier T, Samoska L and Fung A 2007 *IEEE Int. Electron. Devices Meeting* (Washington, USA 10–12 December 2007) p 609

[3] Urteaga M, Pierson R, Rowell P, Jain V, Lobisser E and Rodwell M J W 2011 *Device Res. Conf. (DRC) 69th Annual* (Santa Barbara, USA 20–22 June 2011) p 281

[4] Jin Z, Su Y, Cheng W, Liu X, Xu A and Qi M 2008 *Chin. Phys. Lett.* **25** 2686

[5] Zhou L, Jin Z, Su Y, Wang X, Chang H, Xu A and Qi M 2010 *J. Semicond.* **31** 9

[6] Cai D, Li X, Zhao Y, Liu T, Gao X and Hao Y 2011 *Semiconduct. Technol.* **36** 743

[7] Jin Z, Su Y, Cheng W, Liu X, Xu A and Qi M 2008 *Solid-State Electron.* **52** 1825

[8] Tanaka S, Amamiya Y, Murakami S, Shimawaki H, Goto N, Takayama Y and Honjo K 1997 *Int. Topical Symp. Millimeter Waves* (Kanagawa, Japan 7–8 July 1997) p 27

[9] Cheng W, Jin Z, Yu J and Liu X 2007 *Chin. J. Semicond.* **28** 943

[10] Dahlstrom M and Rodwell M 2004 *IEEE Int. Conf. Indium Phosphide Relat. Mater.* (Santa Barbara, USA May 31–June 4 2004) p 366

[11] Griffith Z 2003 *PhD Dissertation* (Santa Barbara: UCSB)